pH-sensitive membranes prepared with poly(methyl methacrylate) grafted poly(vinylidene fluoride) via ultraviolet irradiation-induced atom transfer radical polymerization

Journal:	*RSC Advances*
Manuscript ID:	RA-ART-06-2014-006368.R1
Article Type:	Paper
Date Submitted by the Author:	19-Aug-2014
Complete List of Authors:	Hua, He; Nanchang Hangkong University, Department of Environmental and Chemical Engineering Xiong, Ying; Shenzhen Graduate School, Peking University, Environment and Energy School Fu, Cai; Nanchang Hangkong University, Department of Environmental and Chemical Engineering Li, Na; Nanchang Hangkong University, Department of Environmental and Chemical Engineering

Paper

pH-sensitive membranes prepared with poly(methyl methacrylate) grafted poly(vinylidene fluoride) via ultraviolet irradiation-induced atom transfer radical polymerization

Helin Hua[a], Ying Xiong [b,*], Caijie Fu[a] and Na Li [a,*]

Ultraviolet (UV) irradiation induced atom transfer radical polymerization (ATRP) was performed to graft poly (methyl methacrylate) (PMMA) on poly(vinylidene fluoride) (PVDF) and got copolymer (PVDF-g-PMMA). Under UV irradiation, the polymerization not only occurred at room temperature, but also achieved a 24% conversion rate only after 120 min exposure. The result of gel permeation chromatography (GPC) indicated that the molecular weight range of the copolymer was narrow, and the UV-induced ATRP was controlled. The PVDF-g-PMMA copolymer was as an additive blending with PVDF to produce a series of novel pH-sensitive microfiltration membranes. With an increase of the copolymer ratio in the membranes, the hydrophilicity of MF membranes increased and exhibited excellent water flux. The water flux of the pure PVDF-g-PMMA MF membrane was about ten times as that of a pure PVDF membrane at pH 7. And the blend membranes showed an excellent sensitivity with pH.

1. Introduction

Stimuli-responsive membranes can exhibit remarkable property changes in response to slight changes in the surrounding environment, such as pH,[1, 2] temperature,[3] ionic strength [4, 5] and others.[6-8] Because of these unique properties, they have considerable potential application in sensors, water treatment and drug delivery. Functionalized pH-sensitive membranes can be prepared by surface grafting 'sensitive' monomers, such as acrylic acid and methacrylic acid [9, 10] onto prepared membranes. However, surface-grafting methods directly onto the as-prepared membrane may be accompanied by changes in membrane pore size and its distribution, leading to reduced permeability. To overcome these obstacles, grafting the functional monomers to the pristine material before the fabrication of membranes offers an effective approach to obtain pH sensitive membranes.[11, 12]

Atom transfer radical polymerization (ATRP) is currently one of the most commonly used synthetic polymerization methods to prepare well-defined polymers with complex architecture.[13, 14] ATRP uses a transition-metal catalyst in a low oxidation state to activate an alkyl halide and generate a radical and the catalyst in a higher oxidation state. It can synthesize polymers with a predetermined molecular weight and narrow molecular-weight distribution by the equilibrium maintained between an active and a dormant chain via a reversible deactivation mechanism. But ATRP still faces many problems in that for the high catalyst loadings needed to maintain a reasonable reation rate, the reaction occurs under high temperature conditions, and the polymerization rate is usually slow.[15, 16]

Photopolymerization is an effective way to sythensize polymers. In our team's previous study, the copolymers of polysulfone-graft-acrylic acid and poly(vinylidene fluride)-graft-poly(methyl acrylate) were synthesized by UV-induced graft copolymerization.[17, 18] The photochemical process has some advantages, such as low activation energy, fast reaction speed and low reaction temperature. [19]

According to the advantages of ATRP and photopolymerization, many researchers have worked on photochemically initiated ATRP, [20-22] which is mainly based on photochemical generation of an activator in the ATRP and combines the advantages of photochemistry and ATRP. Konkolewicz [20] found that photoinduced ATRP of acrylates and methacrylates can be performed at catalyst loadings as low as 100 mg/L using visible light and sunlight. In the presence of light, the polymerization is initiated after the photoreduction of a Cu^{II} complex to a Cu^{I} complex. Furthermore, there was an increase in the reaction rate when shorter irradiation wavelengths were used.

In this study, it is demonstrated that hydrophilic side chains can be grafted onto the secondary halogenated sites of PVDF by a photo-induced ATRP method and hence achieve the synthesis of a PVDF-g-PMMA copolymer. A series of pH-sensitive filtration membranes were prepared by adding a certain quantity of the PVDF-*g*-PMMA copolymer as an additive into the casting solution. In this study, the pH responsiveness of the membranes was investigated.

2. Experimental

2.1. Materials

Poly (vinylidene fluoride) (PVDF) was purchased from Shanghai 3F New Materials Co. Ltd., Methyl methacrylate (MMA), copper(I) bromide (CuBr), 2,2-dipyridyl (bpy, 99%), Poly(vinylpyrrolidone) (PVP), trifluoroacetic acid (TFA), formic acid, 1-methyl-2-pyrrolidinone (NMP, reagent grade), *N*,*N*-dimethylacetamide (DMAc), ethanol and methanol were purchased from Aldrich Chemical Co., and used directly.

2.2. Synthesis of PVDF-*g*-PMMA copolymers by UV-induced ATRP

Proper PVDF was dissolved in 50 mL NMP in a self-made quartz vessel with stirring until the PVDF dissolved. Then bpy and MMA were added into the mixture, and degassed by purging argon. After that, CuBr was added into the reactor and purged with argon gas for 30 min to remove oxygen. The vessel was sealed and put into a UV reactor, which contained a 1 kW medium-pressure mercury lamp with maximum emission at 365 nm and an irradiance of 20 mW/cm^2 at the vessel. The space between the lamp and the vessel was 20 cm. The mixture was stirred and reacted at ambient temperature under the UV light for a predetermined exposure time. After that, the resulting mixture was precipitated by a water/ethanol (1:1 v/v) mixture, and extracted into chloroform for 24 h. This procedure was repeated three times in order to remove unreacted MMA monomer and the resulting MMA homopolymer. The purified product was a grafted copolymer PVDF-*g*-PMMA and was dried for 24 h under vacuum at 80 ^{o}C. Scheme 1 shows the grafting reaction.

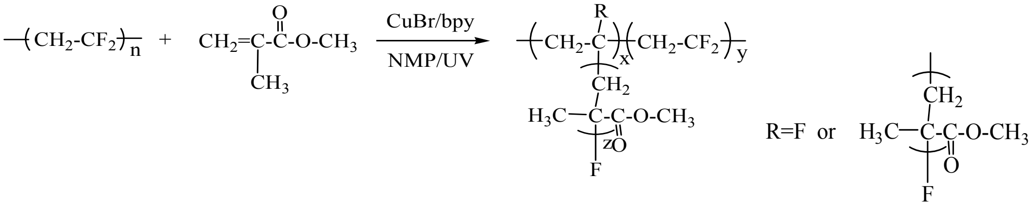

Scheme 1 Synthesis of the PVDF-*g*-PMMA graft copolymer

The grafting conversion of MMA was calculated according to the following Equation 1:

$$\text{Conversion rate (\%)} = \frac{m_1 - m_0}{m} \times 100\% \tag{1}$$

where m_1 and m_0 were the masses of grafting copolymer and initial PVDF, and m is the initial mass of MMA.

2.3. Preparation of pH-sensitive membranes

PVP was used as an additive and dissolved in DMAC. With the total concentration of the membrane solution was constant as 20 wt%, the different amounts of PVDF-*g*-PMMA and PVDF were added into the mixture solution to produce membrane casting solutions. The compositions of the different membrane casting solutions are illustrated in **Table 1**. The M-1 membrane was the pure PVDF membrane and M-5 is the pure PVDF-g- PMMA membrane. Membranes were cast in air (temperature: 25 ± 1 °C, humidity 35-45%) on a glass plate using a glass knife. After a 30 s delay, the glass plate was immersed in de-mineralized water. After 15 min, the membrane was peeled from the glass plate and then immersed in de-mineralized water for 24 h.

Table 1 Composition of various membrane casting solutions

Membranes	DMAc(mL)	PVDF(g)	PVDF-g-PMMA(g)
M-1	50	10	0
M-2	50	7.5	2.5
M-3	50	5	5
M-4	50	2.5	7.5
M-5	50	0	10

The produced membranes were immersed into a mixture of TFA and formic acid (v/v =1:4) for 24 h to cleave the –OCH_3 groups and generate carboxylic acid groups at ambient temperature according to the literature.[23] Then the membranes were taken out of the solution and washed with water. After this acidification process, a series of pH sensitive membranes with poly(methacrylic acid) （PMAA） chains were prepared and the blended membranes were PVDF/PVDF-g-PMAA membranes. Scheme 2 shows the conversion of the membranes.

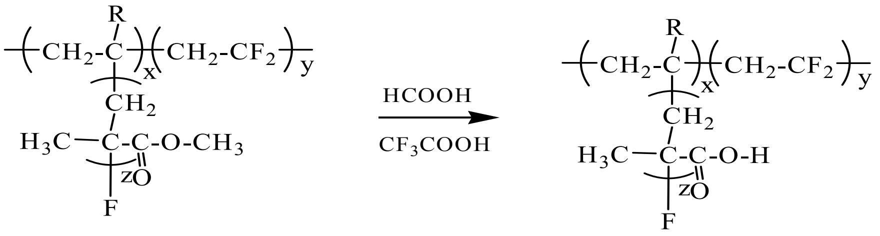

Scheme 2. Acidification of membranes

2.4. Characterization of PVDF-g-PMMA copolymer and membranes

Gel permeation chromatography (GPC) of PVDF and PVDF-*g*-PMMA copolymers was conducted at 30 °C in DMF containing 1% lithium nitrate at a flow rate of 1 mL/min, using a Waters 510 HPLC pump, Waters Styragel columns, and a Waters 410 differential refractometer (Millipore Corp., Bedford, MA).

The chemical composition of the copolymer was determined by a Nicolet Avatar 360 ATR/FTIR spectroscopy and x-ray photoelectron spectroscopy (XPS, Kratos Co, UK). The XPS measurements were performed on a Kratos AXIS Ultra spectrometer using monochromatic Al Kα (1486.71 eV) as the radiation source.

The surface and cross-section morphologies of the pH-sensitive membranes were examined by scanning electron microscopy (SEM, JSM-6301F). The SEM measurements were performed at an accelerating voltage of 5 kV at 20 ^{o}C.

2.5. Pore size measurement

Using a home-made apparatus, the membrane pore sizes were measured using the bubble point analysis method. Before the measurement, the membranes were immersed in aqueous solution at pH = 7.0 for 24 h. Then the membranes were kept in ethanol for 30 min to open all membrane pores. A pretreated membrane was mounted on a sample holder with an effective area of 10.8 cm^2 in a sealed container. Nitrogen gas was charged and the gas pressure increased slowly and continuously. When the first bubble on the surface of the membrane was observed, the gas pressure was recorded, which indicated the maximum pore size. When the last bubble was observed on the surface of membrane, the highest pressure was recorded as an indication of the minimum pore size. The average value of the maximum pore size and the minimum pore size was recorded as the mean pore size.

The results are governed by the Washburn equation as the Equation 2: [12]

$$Pr = 2\gamma \cos \theta \qquad (2)$$

where P is the N_2 pressure, r is the average pore radius of the measured membrane, and $\gamma \cos \theta$ is the Wilhelmy surface tension.

2.6. Water flux and pH sensitivity of the membranes

The water flux of the membranes at different pH values was investigated with a home-made microfiltration cell apparatus. The membranes were immersed in aqueous solutions at a certain pH overnight before the test. Then they were mounted on a microfiltration cell with an effective area 10.8 cm^2 and compacted at 0.1 MPa for 30 min. An aqueous solution with same pH was added into the cell and stirred at 600 rpm under a nitrogen atmosphere at a pressure of 0.1 MPa. The water flux was calculated from the volume of permeating solution per unit time and per unit area of the membrane surface.

2.7. Diffusional permeation of the membranes

The diffusional permeability experiments of the pH-sensitive membranes were performed using a standard side-by-side diffusion cell. The membrane sample was cut into a square with an effective permeation area of 10.75 cm^2 and immersed in the permeant solution overnight before the diffusional experiments. 60 mL solutions with the same pH were added simultaneously to the receptor and donor cells, respectively. VB_{12} and KCl were chosen as the solutes. The initial concentrations of VB_{12} and KCl in the donor side were 0.1 mg/mL and 0.01 mol/L, respectively. Deionized water was used in the receptor compartment. The concentration of VB_{12} was determined with a UV–vis Spectrometer (Spectrumlab 54, Lengguang, Shanghai) at 360 nm. And the concentration of KCl was determined by measuring the electrical conductance with an electrical conductivity meter (DDS-307, Shanghai) and probe (DJS-1C, Shanghai).

The diffusion coefficient of solute across the membrane was calculated from the following Equation 3 derived from Fick's first law of diffusion: [31, 32]

$$D = \frac{1}{2} \times V \times \frac{L}{A} \times \frac{1}{t} \times \ln \frac{C_f - C_i}{C_f - C_t} \qquad (3)$$

where D is the diffusion coefficient (cm^2 s^{-1}); C_i, C_t and C_f are the initial, intermediate (at time t), and final concentrations of solute in the receptor side, respectively (M); V is the effective volume of a compartment (cm^3); L is the thickness of the dry membrane (cm); A is the effective diffusional area (cm^2) of the membrane.

3. Results and discussion

3.1. Graft polymerization kinetics study

A series of ATRP experiments were performed to study the polymerization process of PVDF-g-PMMA. **Fig. 1** shows the kinetic plots and changes of the conversion rate with UV exposure time. Plots of ln ($[M]_0/[M]$) versus exposure time exhibited a good linear relationship, which indicated that the polymerization exhibited a first-order reaction dynamic mode. In the whole ATRP process, the concentration of activator maintained constant and controlled the ATRP. With increasing exposure time, the conversion rate increased and the maximum conversion rate achieved 24% when the exposure time was 120 min.

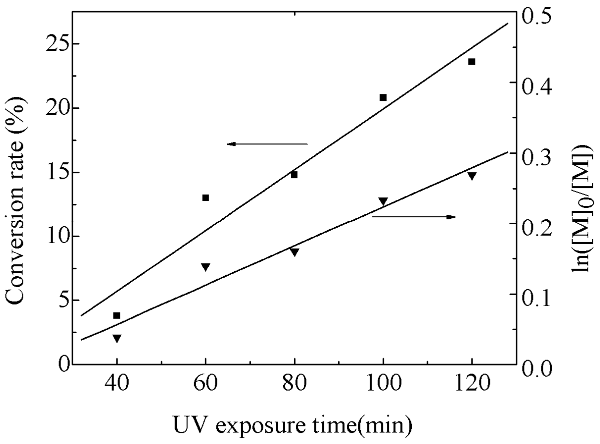

Fig. 1 Kinetic plot and conversion rate of MMA as a function of UV exposure time

In the literature, Sebnem[24] also synthesized PVDF-g-PMMA by the ATRP method operating at 60 or 90 °C. When the conversion rates were 17% and 25%, the reaction conditions were at 60 °C for 240 min and at 90 °C for 30 min. Hester[25] synthesized PVDF-g-PtBMA by the ATRP method and hydrolyzed the resulting polymer to yield PMAA. The ATRP reaction was performed at 90 °C for 20 h. These data indicated that PMMA grafting onto PVDF by ATRP method occurred at high temperature. Under UV light, the air-stable Cu^{II} complex reduces and yields a Cu^{I} complex. This initiates the ATPR reaction of MMA. Compared with the above studies, the application of UV light not only accelerated the polymerization of PVDF-g-PMMA, but also optimized the reaction conditions, which was in accordance with the literature.[26] The UV-initiated ATRP method gives a simple pathway to introduce the hydrophilic MMA side-chain onto the hydrophobic backbone, such as PVDF.

In the following experiments, the PVDF-g-PMMA with the maximum conversion rate 24% was used to detect the copolymer’s character and prepare PVDF/PVDF-g-PMMA blended membranes.

Fig. 2 shows that with increasing conversion rate, the relative molecular mass of the polymer (M_w) increased, while the polydispersity (M_w/M_n) of the polymers exhibited downward trends. **Table 2** shows the results of polymerization with a 120 min UV exposure. A copolymer with a molar mass of 11.92 × 10^5 was obtained. The polydispersity index (PDI) of polymerized PVDF-g-PMMA was 1.83, which was narrow and indicated the controllability of the UV-induced ATRP.

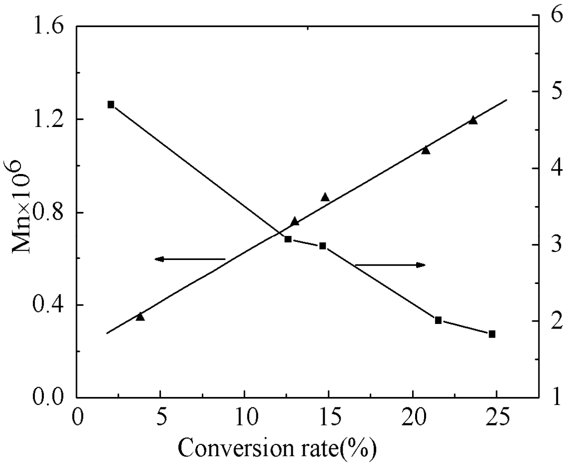

Fig. 2 Evolution of the molar mass and Mw/Mn with the conversion of MMA

Table 2 GPC results of PVDF and PVDF-g-PMMA

	Mn×10^5	Mw×10^5	Mp×10^5	Mz×10^6	Mw/Mn
PVDF	2.18	120.87	21.69	521.71	55.40
PVDF-g-PMMA[a)]	11.92	21.85	6.69	5.64	1.83

[a)] Reaction conditions: [bpy]:[CuBr]:[PVDF]:[MMA]=2:1:1:50; UV irradiation time = 120 min; GPC, based on polystyrene standards

3.2. Characterization of the PVDF-g-PMMA copolymer

Fig. 3 shows the ATR-FIR spectra of pristine PVDF and the resulting PVDF grafted PMMA (PVDF-g-PMMA). Two characteristic peaks appear, one at 1404 cm^{-1} attributed to CH_2 stretching and the other at 1174 cm^{-1} attributed to CF_2 stretching vibration, were observed in the spectra of both PVDF and the PVDF-g-PMMA polymers.[27] Compared to the PVDF spectrum, a new absorption peak at 1739 cm^{-1} was found for PVDF-g-PMMA, which corresponds to the stretching of the carbonyl group on PMMA.[28, 29] The spectral results showed that the PMMA was successfully grafted onto the structure of PVDF.

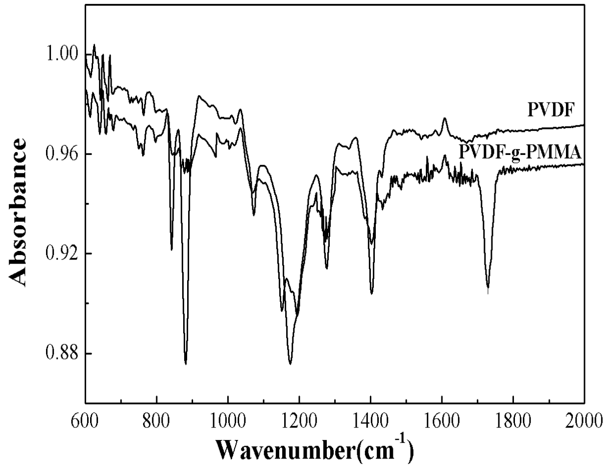

Fig. 3 FT-IR spectra of PVDF and PVDF-g-PMMA

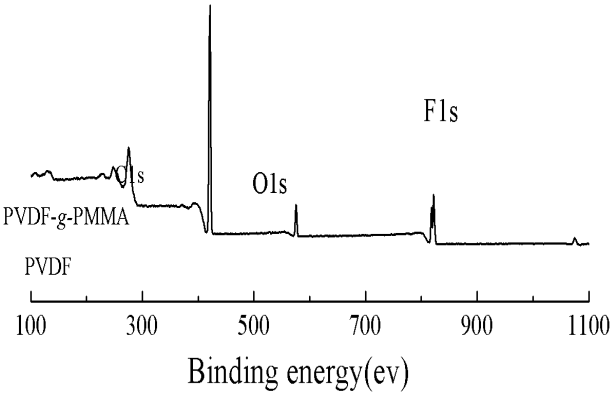

Fig. 4 XPS survey scan spectra of PVDF and PVDF-g-PMMA

Fig. 4 shows the whole XPS spectra of PVDF and PVDF-g-PMMA. Compared to PVDF, a clear O1s band appeared in the PVDF-g-PMMA spectrum, which is attributed to the O atom in PMMA. The C1s core-level spectra of PVDF and

PVDF-g-PMMA are shown in **Fig. 5a** and **5b**, respectively. In Figure 5a, the binding energies at 290.93 eV and 286.43 eV are assigned to the C-F and C-C/H bands, respectively, on the PVDF main chains.[25] The C 1s spectrum of the PVDF-g-PMMA copolymer can be curve-fitted into four peak components. The binding energies of the four composition components are centered at 284.54, 286.34, 288.64 and 290.24 eV, respectively, corresponding to the chemical bonds of C-C or C-H, C-O, O-C=O and C-F. The above results also indicate that PMMA had successfully grafted onto the main structure of PVDF.

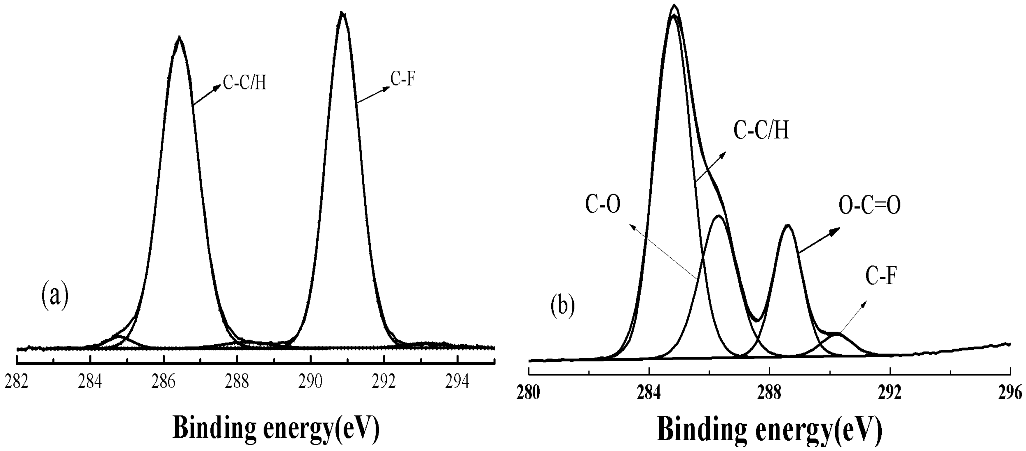

Fig. 5 C 1s spectra of PVDF (a) and PVDF-g-PMMA (b)

3.3. Morphology of the membranes

SEM micrographs of the cross sections and surfaces of membranes with different fractions of PVDF-g-PMMA are shown in **Fig. 6(b-e)** and **(b'-e')**. Compared with the morphology of the PVDF/PMMA blended membrane, [28, 30, 31] there were no spherulitic structures of PVDF or phase separation in the cross-sections of all PVDF/PVDF-g-PMMA blended membranes, which indicates that the PVDF-g-PMMA and PVDF copolymers were compatible. In Fig. 6, there were also finger-like porous structures through the membrane cross-sections and higher surface porosity on the surface morphology. Also the volume of macrovoids increased with increasing amount of PVDF-g-PMMA. The reason can be attributed to the enhanced hydrophilicity of PVDF-g-PMMA which resulted in a longer time for the solvent exchange between the water bath and the polymer solution. The longer the time for the solvent exchange, the more developed are the processes of polymer-lean phase growth and coalescence; hence the larger porous structure.[12]

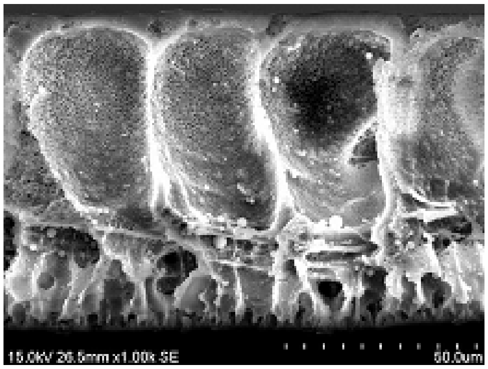

a

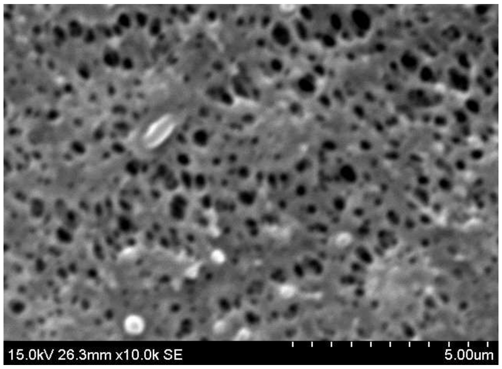

a’

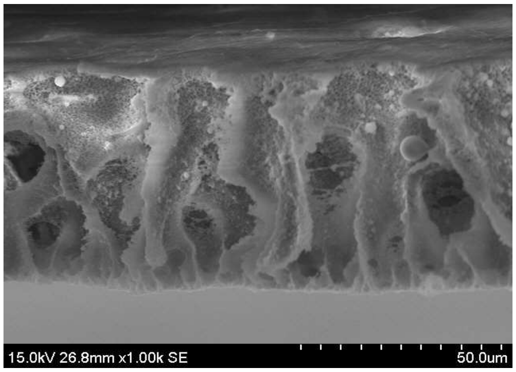

b

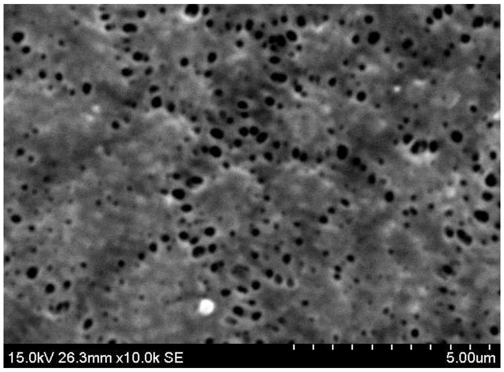

b’

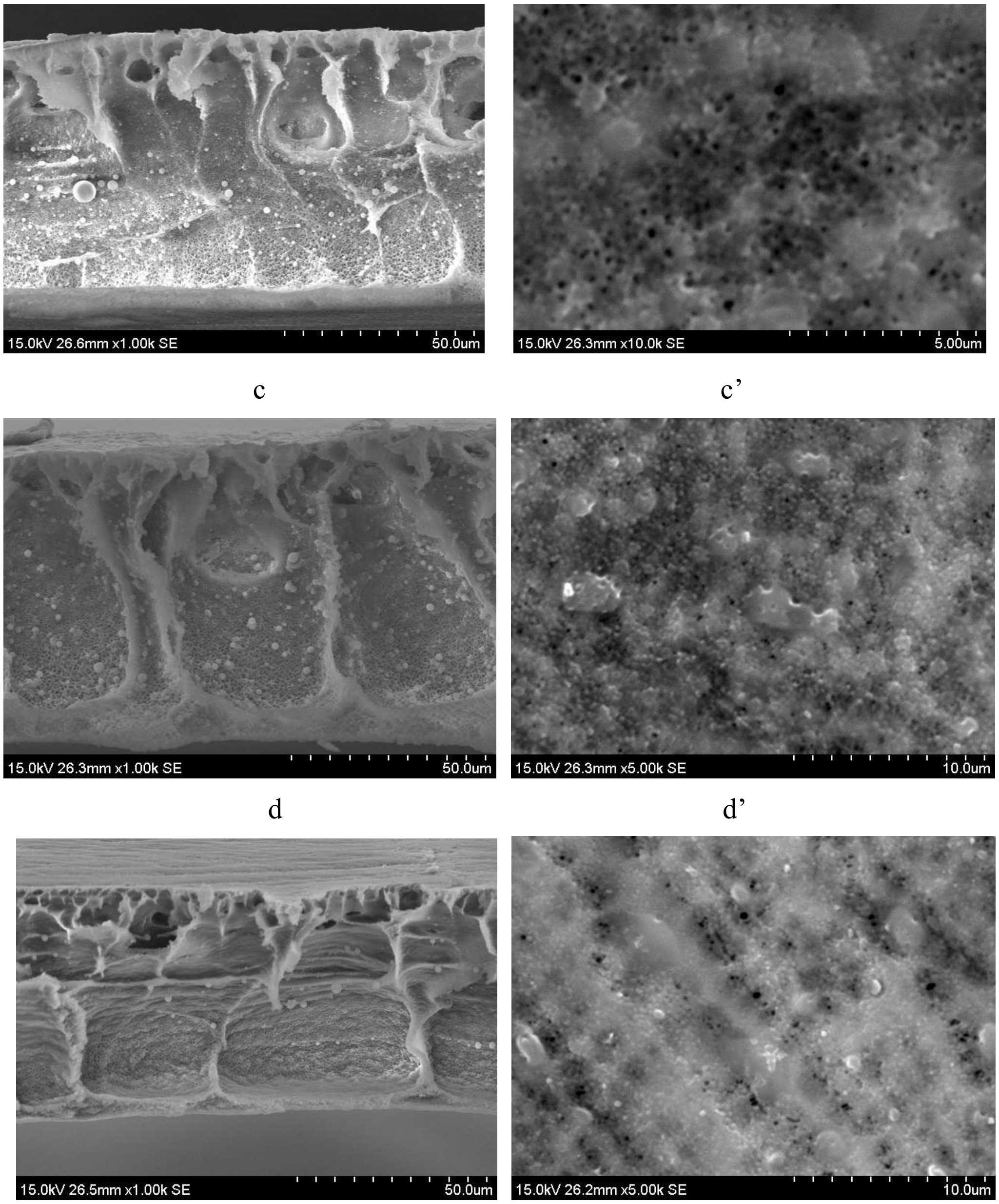

c c'

d d'

e e'

Fig. 6 SEM images of cross-sections (a-e) and surfaces (a'-e') of various membranes (a) M-1, (b) M-2, (c) M-3, (d) M-4, (e) M-5

The structure of the blended membranes affected the water flux and permeation of the membranes. The grafting of PMMA onto the PVDF backbone was an effective method to enhance PVDF's hydrophilic performance. In the membrane preparation process, the total polymer concentration was constant as 20%. Thus, the PVDF concentration of the blend membranes decreased with the increasing addition of the copolymer PVDF-g-PMMA. And the addition of the copolymer PVDF-g-PMMA enhanced the performance of the blended membranes, which will be discussed in the following sections.

3.4. Water flux and mean pore size of the PVDF/PVDF-g-PMAA membranes

The effects of the PVDF-g-PMAA copolymer addition on the membrane pore size and flux are shown in **Fig. 7** at pH 7.0. The flux increased with increasing of copolymer content. The M-5 membrane, which is the pure PVDF-g-PMAA membrane, had the maximum water flux as 1300 L m^{-2} h^{-1} and it was 13 times of that of the pure PVDF membrane.

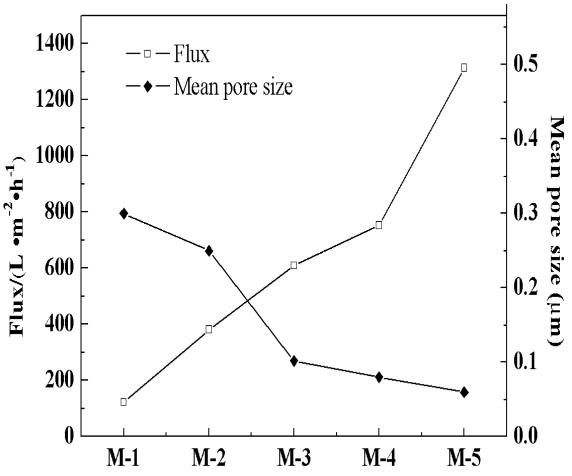

Fig. 7 Water flux and mean pore size of different membranes at pH=7.0

However, the membrane pore size decreased with increasing copolymer content, which was consistent with the surface SEM results in section 3.4. The carboxyl groups of PMAA were sensitive to the solution pH, which would affect the pore size of the membranes. So there were the more PVDF-g-PMMA in the membrane the more influence on the membrane pore size. And the influence of pH on the different membranes would be discussed in Section 3.5.

In the filtrtion process, there are two factors which affect the water flux.[12] One is the membrane pore size and another is the hydrophilicity of the membranes. According to the above results, the increased water flux was arributed to an increased hydrophility of the membranes, which was attributed to the hydrophilic chain PMAA grafted onto the structure of PVDF.

3.5. Hydraulic permeation

The membrane hydraulic fluxes under various pH conditions are shown in **Fig. 8**, which shows that the PVDF/PVDF-g-PMAA membranes had obvious sensitivity to pH between pH 3 and 12. The water flux of pure PVDF membranes remained stable at about 124-130 LMH ($L\cdot M^{-2}\cdot h^{-1}$) as the pH varied. However, the membrane water fluxes with different contents of PVDF-g-PMMA were dependent on the pH, and the flux deceased with increasing pH. Among these membranes, the pure PVDF-g-PMAA membrane with a 20% content had the highest water flux. With the pH increasing from 3 to 12, the water flux decreased from a maximum 3408 LMH at pH = 3 to a minimum of 398 LMH at pH = 12.

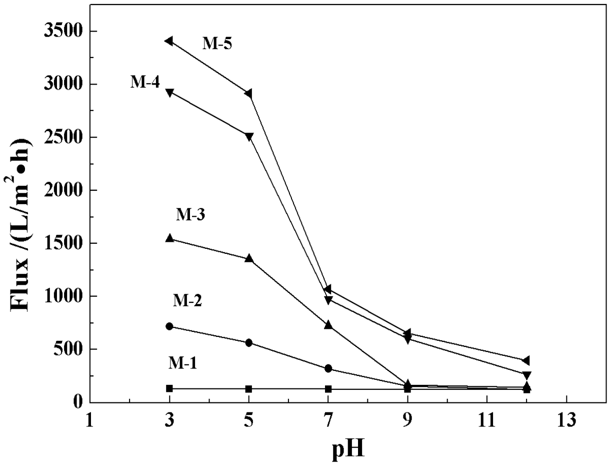

Fig. 8 pH dependence of water flux for the various membranes

The pH dependance was attibuted to the extension of the grafted PMAA chains. When pH value was lower than the pK_a of PMAA (about pH=6.15), [32, 33] the carboxyl groups of PMAA was protonated and reduced the electrostatic repulsion within the PMAA chain. It made the membrane pore to maintain "open" state. When pH value was higher than the pK_a of PMAA (about pH=6.15), the carboxyl groups of PMAA were negatively charged. The repulsion between negative charges made the PMAA chains extended, which caused the membrane pore decreasing and being as "close". The test results that the range of water flux decrease was the largest from pH = 5 to 7 also proved this theoretical analyses.

3.6. Diffusional permeability study

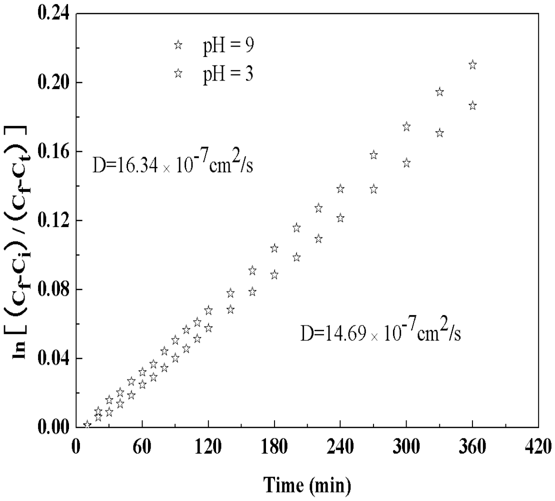

Fig. 9 Effect of pH on the diffusional permeation of VB_{12} through the membrane M-3

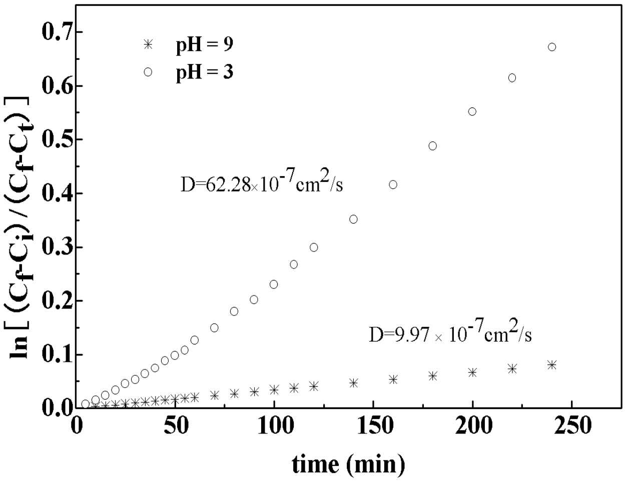

Fig. 10 Effect of pH on the diffusional permeation of KCl through the membrane M-3

In order to investigate the concentration-driven solute diffusion behavior across the pH-sensitive membranes, KCl and VB_{12} were selected as solutes with various concentrations at various pHs, respectively. The M-3 membrane, which has the same content PVDF and PVDF-g-PMMA polymer in the membrane, was chosen for the testing. **Fig. 9** and **Fig. 10** reveal the diffusional behavior of VB_{12} and KCl through the M-3 membrane at pH 3 and 9. A plot of $\ln[(C_f\text{-}C_i)/(C_f\text{-}C_t)]$ against time t is shown in each figure, and the permeability coefficients of VB_{12} and KCl at pH 3 and 9 were calculated.

The permeability coefficients of VB_{12} and KCl at pH 3 and 9 were calculated and shown in Fig. 9 and Fig. 10, respectively. The data indicated that the permeability coefficients of two solvents decreased with the increasing of pH, which was the same as that of the PES-C-grafted-PMAA membrane.[32] The VB_{12} molecule is about 2.09nm, [34] which was smaller than the produced membranes pore size at pH 3 and 9. So the resulting permeability coefficients do not represent a remarkable response.

The KCl dissociates as K^+ and Cl^- ions when it is dissovled in water. With the same as the VB_{12} molecule, the ions were also smaller than the produced membrane pore size. But it gave a different permeability according to the change of pH. When the pH was increased from 3 to 9, the KCl diffusion permeability decreased dramatically. This result was attributed to the joint action of two aspects. One is the reduced pore size caused by the extension of PMAA chains when pH decreases. Another is the electrostatic interaction by dissociation of carboxyl groups on PMAA, [32] which is the major role. When pH was 9, the carboxyl groups of the PMAA chains were negatively charged. Then when the ions diffused the membrane pore, they would be obstructed with electrostatic repulsion effects the by the negatively charged PMAA chains. So the PVDF/PVDF-g-PMMA membranes could use to separate salt under different pH condition.

4. Conclusions

PVDF-g-PMMA was synthesized by UV irradiation-induced ATRP. UV exposure accelerated the ATRP process at room temperature and caused a controlled radical polymerization of PVDF-g-PMMA. The maximum conversion rate was 24% when the exposure time was 120 min. By ATR-FIR and XPS measurements, it was found that the PMMA was successfully grafted onto the structure of PVDF. This UV-induced ATRP offers an effective way to prepare the copolymers based on PVDF.

A series of pH-sensitive membranes were prepared by blending PVDF-g-PMMA and PVDF powders. SEM micrographs revealed that PVDF-g-PMMA and PVDF were quite compatible. When the membrane is the pure PVDF-g-PMMA, a maximum water flux of 3408 L m^{-2} h^{-1} was observed at pH 3. The blended membranes also exhibited an obvious pH-response performance. The addition of PVDF-g-PMMA increased the hydrophilicity of the blended membranes.

---

[a] Department of Environmental and Chemical Engineering, Nanchang Hangkong University, Nanchang 330063, P. R. China, E-mail: xueimpossible@sohu.com

[b] School of Environment and Energy, Shenzhen Graduate School, Peking University, Shenzhen Key Laboratory for Metal Pollution Control and Reutilization, Shenzhen 518055, P. R. China, E-mail: xiongying@iee.pku.edu.cn

ACKNOWLEDGEMENTS

The authors would like to thank the financial support from Shenzhen Science and Technology Research fund basic research program (JC201105170738A), Jiangxi Province National Science Foundation (2010GQH0109) and Project of Education

Department of Jiangxi Province (GJJ11525). The authors are grateful to Prof. James R. Bolton from the Department of Civil and Environmental Engineering at the University of Alberta for his kind assistance with our English writing.

REFERENCES

1 C.Cheng, L. Ma, D.F. Wu, J. Ren, W.F. Zhao, J.M. Xue, S.D. Sun and C.S. Zhao, J. Membr. Sci. 2011, 378, 369-381.

2 Z.H. Yin, K.Y. Fu, J. Gao, X.L. Cao, L.L. Li and C.S. Zhao, J. Appl. Polym. Sci. 2011, 119, 3607-3614.

3 H.Y. Yu, W. Li, J. Zhou, J.S. Gu, L. Huang, Z.Q. Tang and X.W. Wei, J. Membr. Sci. 2009, 343, 82-89.

4 J.L. Shi, L.F. Fang, H. Li, H. Zhang, B.K. Zhu and L.P. Zhu, J. Membr. Sci. 2013, 437, 160-168.

5 Z. Liu, F. Luo, X,J, Ju, R. Xie, T. Luo, Y.M. Sun and L.Y. Chu, Adv. Funct. Mater. 2012, 22, 4742-4750.

6 M. Yang, L.Y. Chu, H.D. Wang, R. Xie, H. Song and C.H. Niu, Adv. Funct. Mater. 2008, 18, 652-663.

7 L.Y. Chu, Y. Li, J.H. Zhu, H.D. Wang and Y.J. Liang, J. Controlled Release 2004, 97, 43-53.

8 C.J. Sheng, S. Wijeratne, C. Cheng, G.L. Baker and M.L. Bruening, J. Membr. Sci. 2014, 459, 169-176.

9 J.F. Hester, S.C. Olugebefola, A.M. Mayes, J. Membr. Sci. 2002, 208, 375-388.

10 Y. Osada, K. Honda, M. Ohta, J. Membr. Sci. 1986, 27, 327-338.

11 L.L. Li, Z.H. Yin, F.L. li, T. Xiang, Y. Chen, C.S. Zhao, J. Membr. Sci. 2010, 349, 56-64.

12 B. Deng, X.X. Yang, L.D. Xie, J.Y. Li, Z.C. Hou, S. Yao, G.M. Liang, K.L. Sheng, Q. Huang, J. Membr. Sci. 2009, 330, 363-368.

13 N.V. Tsarevsky, K. Matyjaszewski, Chem. Rev. 2007, 107, 2270-2299.

14 K. Matyjaszewski, Isr. J. Chem. 2012, 52, 206-220.

15 T.E. Patten, J. Xia, T. Abernathy, Science, 1996, 272, 866-868.

16 Y. Bao, X.Z. Yao, J.Z. Ma, Polym. Bull. (China) 2012, 8, 64-73.

17 H.L. Hua, G.X. Wu, N. Li, L.A. Wei, Polym. Mater. Sci. Eng. 2010, 26, 130-133.

18 H.L. Hua, Y.Q. Han, N. Li, G.X. Wu, J.Chem. Eng. of Chinese Univ. 2010, 24, 903-906.

19 Y. Yagci, S. Jockusch, N.J. Turro, Macromolecules, 2010, 43, 6245-6260.

20 D. Konkolewicz, K. Schröder, J. Buback, S. Bernhard, K. Matyjaszewski, ACS Macro Letters 2012, 1, 1219-1223.

21 J. Mosnacek, M. Ilǒíková, Macromolecules 2012, 45, 5859-5865.

22 M.A. Tasdelen, M. Uygun, Y. Yagci, Chem. Phys. 2010, 211, 2271-2275.

23 G.J. Liu, Z.H. Lu, Macromolecules, 2004, 37, 4218-4226.

24 I. Sebnem, C.O. Solar, H.A. Metin, M.M. Annem, Des. Monomers Polym. 2004, 7, 181-189.

25 J.F. Hester, P. Banerjee, Y.Y. Won, A. Akthakul, M.H. Acar, A.M. Mayes, Macromolecules, 2002, 35, 7652-7661.

26 M. Jaroslav, I. Marketa, Macromolecules, 2012, 45, 5859-5865.

27 C.X. Xu, W. Huang, X. Lu, D.Y. Yan, S.T. Chen, H. Huang, Radiat. Phys. Chem. 2012, 81, 1763-1769.

28 S. Rajabzadeh, T. Maruyama, Y. Ohmukai, T. Sotani, H. Matsuyama, Sep. Sci. Technol. 2009, 66, 76-83.

29 Y.H. Ding, P. Zhang, Z.L. Long, Y. Jiang, F. Xu, W. Di, J. Membr. Sci. 2009, 329, 56-59.

30 S. Rajabzadeh, C. Liang, Y. Ohmukai, T. Maruyama, H. Matsuyama, J. Membr. Sci. 2012, 423, 189-194.

31 T. Ma, Z.Y. Cui, Y. Wu, S.H. Qin, H. Wang, F. Yan, N. Han, J.X. Li, J. Membr. Sci. 2013, 444, 213-222.

32 M. Wang, Q.F. An, L.G. Wu, J.X. Mo, C.J. Gao, J. Membr. Sci. 2007, 387, 257-263.

33 Y.M. Lee, S.Y. Ihm, Polymer 1995, 36, 81-85.

34 Z. Guo, G.S. Zhu, M.H. Xin, B. Gao, S.L. Qiu, CHEM. J. CHINESE U. 2006, 27, 9-12.